

Thermal analysis of hydroxyapatite with adsorbed oxalic acid

Ewa Skwarek¹

Received: 20 October 2014 / Accepted: 2 April 2015 / Published online: 13 May 2015
© The Author(s) 2015. This article is published with open access at Springerlink.com

Abstract The specific adsorption of oxalic acid ions at the hydroxyapatite interface was investigated by means of the radioisotope method (^{14}C) as a function of oxalic acid ions concentration, NaCl concentration and pH. Application of hydroxyapatite has become extensive in the bio-material field due to its biocompatibility with human hard tissue. Hydroxyapatite was synthesized using wet methods. Physical properties of the resulting powder were characterized by DTA/TG, XRD, AFM and SEM microscopy. Physicochemical properties characterizing the electrical double layer of the hydroxyapatite/NaCl solution interface were determined. The zeta potential and the adsorption of oxalic acid molecules were studied as a function of pH. The point of zero charge and the isoelectric point of samples were determined: its values are as follows: $\text{pH}_{\text{PZC}} = 7$ and $\text{pH}_{\text{IEP}} = 4$. Temperature has insignificant influence on pure substance and with oxalic acid adsorbed, as thermal analysis has shown, and characterization of hydroxyapatite structure can be carried out by this thermal analysis. Two phenomena are responsible for oxalic acid adsorption: phosphate group replacement at the hydroxyapatite surface by oxalic ions simultaneous to intraspherical complexes formation.

Keywords Hydroxyapatite · Oxalic acid · Adsorption · Thermal analysis

The present article is based on the lecture presented at ICVMTT 34 conference in Kyiv—Ukraine on 20–21 May, 2014.

✉ Ewa Skwarek
ewunias@hektor.umcs.lublin.pl

¹ Faculty of Chemistry, Maria Curie-Skłodowska University, Maria Curie-Skłodowska Sq. 5, 20-031 Lublin, Poland

Introduction

Hydroxyapatite $\text{Ca}_{10}(\text{PO}_4)_6(\text{OH})_2$ (HAP) is the main component in vertebrate hard connective tissues such as teeth and bones. It is also an important component of soils and insects and is used for soil recultivation.

Oxalic acid is a compound common in nature occurring in many plants such as rhubarb, spinach, sorrel and beets. It can cause, among others, kidney stone formation as well as various changes in soil; therefore, it is regarded to be a toxic substance. Oxalic acid is commonly found in water and soil as a natural product of plant, and animal remains decomposition. According to the recent investigations, organic acids change significantly bioavailability of heavy metals in soil and can affect phytoremediation effectiveness [1].

The interaction of organic acids contained in soil with the surface of minerals found that there is an important phenomenon in the natural environment. Due to specific composition, crystalline structure and adsorption properties of hydroxyapatite, a new possibility appears for its application in separation of organic acids [2] and also understanding the effect of oxalic acid influence on removal of different environment contaminants [1, 3]. Therefore, more and more attention is paid to the studies of organic acids effect on hydroxyapatite, and there can be found a few papers devoted to adsorption of oxalic acid on hydroxyapatite. One paper describes two kinds of hydroxyapatite of different degree of crystallinity which was generated by the sol–gel and chemical precipitation methods. The effect of crystallinity on adsorption and hydroxyapatite dissolution properties was studied in it. The results showed that crystallinity had an enormous effect on adsorption and dissolution of hydroxyapatite. Poorly crystallized (degree of crystallinity $X_c = 0.23$) hydroxyapatite has adsorbed

larger amounts of oxalic acids than well-crystallized one ($X_c = 0.86$) [4].

Thermal stability of hydroxyapatite is often investigated in the literature due to methods of hydroxyapatite preparation and following temperature and time of its heating [5–7]. High-temperature processing is essential for the preparation of apatites for biomaterials, lighting, waste removal and other applications. This requires a good understanding of the thermal stability and transitions upon heating. The structural modifications for substitutions are discussed to understand the temperature processing range for different apatites. This is based on a review of the literature from the past few decades, together with recent research results. Apatite thermal stability is mainly determined by the stoichiometry (Ca/P ratio and structural substitutions) and the gas composition during heating. Thermal stability is lowered mainly by a substitution of calcium and phosphate, leading to a loss in phase stability at temperatures lower than 900 °C. The anions in the hexagonal axis, OH in HAp, are the last to leave upon heating, and prevention of these groups loss ensures high-temperature stability. The information discussed here will help to understand the changes of apatites during heating in calcination, sintering, hydrothermal processing, plasma spraying, flame pyrolysis and other high-temperature processes [8]. The literature data concerning the thermal decomposition of hydroxyapatite during sintering are still ambiguous as regards the minimum decomposition temperature, as well as the actual extent and products of the decomposition itself. Some results show that stoichiometric hydroxyapatite is stable in dry or moist air up to 1200 °C and does not decompose. The other authors report that stoichiometric hydroxyapatite, after a dehydroxylation process (which occurs gradually but in two steps, i.e. at about 900 °C and 1300–1400 °C), starts to decompose into secondary phases at the temperature in the range 1350–1500 °C [9].

There are several ways to measure the charge that accumulates on a surface when it absorbs ions from a solution. The principal measure of this charge is the zeta potential, which is common to all methods based on electrokinetic phenomena. However, the zeta potential measures not just the charge on the solid surface but includes the charge in the associated static fluid near the surface (including the double layer). The zeta potential is therefore very useful in the rheology of colloidal solutions and suspensions as well as cement pastes but less meaningful when addressing the chemistry of a surface. A much less common technique is surface titration, where the buffering capacity of a surface is determined by its ability to soak up H^+ (and/or OH^-) from solution in the pH_s range. This technique gives insight into the Breasted acidity and alkalinity of the accessible chemical groups on the surface,

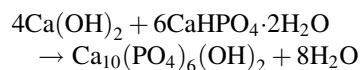
the information that is more relevant to the interactions such as protein adsorption than the data associated with the slip plane of zeta potential measurement. The aim of the study [10] was to use surface titration to determine the surface charge of stoichiometric hydroxyapatite (Ca/P ratio 1.67) and to investigate its behaviour in the presence of physiological levels of Ca^{2+} .

The aim of the paper was to study the effects of oxalate ions on the parameters characterizing a electrical double layer. The obtained material was studied to determine experimental parameters characterizing a double electrical layer, i.e.: density of surface charge and zeta potential dependence on pH and ionic strength of electrolyte, amount of oxalate ions adsorption in a pH function and their concentration in the NaCl solution, effect of the presence of oxalate ions on surface charge density and zeta potential in the hydroxyapatite/NaCl system, as well as to thermal analyse of oxalic acid adsorbed on hydroxyapatite.

Materials and methods

Synthesis of HAP

Synthetic hydroxyapatite for experiments was prepared using the hydrothermal method [11]. The simplified scheme of hydroxyapatite synthesis is as follows:



The procedure for its preparation is as follows: 1.03 g $CaHPO_4 \cdot 2H_2O$ and 0.296 g of $Ca(OH)_2$ were weighed and mixed, then 0.08 dm³ of water was added, and pH value was reduced to 9 using 80 % acetic acid. The synthesis was conducted in the autoclave, then in the dryer for 24 h at 120 °C. The prepared hydroxyapatite required purification. It was washed with double-distilled water and centrifuged to obtain material of the lowest conductivity constant achieving about 13.8 μS. Such material was used for further investigations.

Methods

The thermal analysis of the studied systems was made using a derivatograph Q-1500D (MOM, Hungary). The aim was to investigate the sample mass change depending on temperature (TG, DTG and DTA).

X-ray diffraction was studied by means of the Epyrean diffractometer produced by PANalytical (lamp Cu LEF HR, detector pixel-3D, active channels 255). Porous structure parameters were determined using the traditional method which is low-temperature nitrogen adsorption–desorption measured on AUTOSORB—1CMS produced

by Quantachrome Instruments (USA). The surface was characterized using an electronic microscope S/TEM with the analysis EDX (Titan3TM G2 60-300) and atomic force microscope AFM produced by Veeco (USA) NanoScope V. Size of beads was measured using the device Mastersizer 2000 produced by the Malvern Instruments. The real dispersion state in hydroxyapatite/electrolyte system in 25 and 37 °C and for hydroxyapatite/electrolyte/oxalic acid in the same temperatures was measured in Turbiscan Lab^{expert}.

The surface charge density at the hydroxyapatite/electrolyte solution interface was determined by potentiometric titration of the suspension. The measurement was carried out in a thermostated Teflon vessel, under nitrogen atmosphere free of CO₂, at 25 °C. Measurements of pH were carried out using a PHM 240 Radiometer Research pH meter with K401 as a glass electrode and G202B as a reference calomel electrode. Potentiometric titration was carried out with the use of the automatic burette Dosimat 665 (Metrohm). The whole experiment was controlled by computer software. Potentiometric titration as well as electrokinetic measurements was made at three different concentrations: 0.001, 0.01 and 0.1 mol dm⁻³ of NaCl solutions. The initial concentrations of oxalic acid were 0.000001, 0.00001, 0.0001 and 0.001 mol dm⁻³. All the solutions were prepared with double-distilled water. All the reagents used for experiments were of analytical grade purity.

The zeta potential of the hydroxyapatite was determined by electrophoresis using a Zetasizer 3000 Standard (Malvern). The concentration of hydroxyapatite in the electrolyte solution was 100 ppm. Before measurements, the suspension of hydroxyapatite was ultrasonicated.

The adsorption density at the hydroxyapatite/electrolyte solution interface was measured using the radiotracer technique. The oxalic acid solutions were labelled with ¹⁴C isotope. The adsorption of oxalic acid was studied by determining the changes in radioactivity of the solution with the use of potentiometric titration setup. A predetermined volume of the electrolyte solution (50 cm³ 0.001 mol dm⁻³ NaCl) was placed (at 25 °C) in a Teflon vessel, to which 0.2 cm³ HCl was added afterwards. Inert atmosphere was provided by passing nitrogen over the solution. The solution of electrolyte of the required ionic composition and concentration of oxalic acid was then treated with the solution containing oxalic acid labelled with ¹⁴C. In order to determine the initial activity, three samples of the solution (100 µl volume each) were taken as the zero samples. After equilibrium conditions were obtained (constant temp. of 25 °C and pH of the solution), a weighed sample of oxide (1 g) was added. A computer, controlling the process on the basis of pH meter values, dosed successive portions of 0.1 mol dm⁻³ NaOH

solutions and determined the moment of taking the samples that should demonstrate the course of adsorption on the oxide surface. At that time, a 0.5-cm³ portion of the suspension was taken and the precipitate was centrifuged. Two 100 µL samples of the centrifuged suspension were then taken and added to the containers with 3 mL of liquid scintillator Insta Gel Plus (PerkinElmer Life And Analytical Sciences, Inc, USA). The pulses were then counted using a scintillation counter Beckman LS-5000 DT (Beckman, USA). The adsorption of ions was studied in the pH range 3–11. Adsorption experiments were carried out with radio-labelled oxalic acid (ARC American Radiolabelled Chemical Inc., USA).

Results and discussion

Table 1 presents the results of XRD analysis for hydroxyapatite prepared by the wet method [11], where the values characteristic for the crystalline form of hydroxyapatite can be observed. After adsorption of oxalic acid on the hydroxyapatite surface, no calcium oxalate was found and the obtained quantities were the same as in Table 1. According to the analysis, hydroxyapatite constitutes 98.4 % of the sample when oxalic acid is 1.6 %. It was confirmed by the size of crystallites estimated by means of the Scherrer method after adsorption of oxalic acid on hydroxyapatite—obtained values were 61.39 nm and for pure one 37.31 nm. The adsorbent is of fine crystalline structure. The photo (Fig. 1) presents the hydroxyapatite surface structure. As can be seen, the surface of the samples is not smooth, and there can be seen areas of crystallites. Therefore, nonhomogeneity of acidic–basic properties of surface groups can be expected. The morphology of powder A, B is shown in Fig. 2a, b which is in agreement with particle size distribution determined by sedimentography: powders A and B are characterized by larger agglomerates (3 ± 4 µm) in turn, formed by smaller primary particles (20 ± 30 nm) with respect to powder A, in which grains are smaller but built by larger particles. The specific surface area of the two powders results 35.37 and 23.24 m² g⁻¹ for A and B, respectively. As expected, the compaction behaviour of the

Table 1 XRD characterization

| 2θ | Intensity/% |
|-------|-------------|
| 20 | |
| 25.9 | 35 |
| 31.75 | 100 |
| 32.96 | 55 |
| 39.84 | 20 |
| 46.7 | 40 |
| 49.5 | 30 |

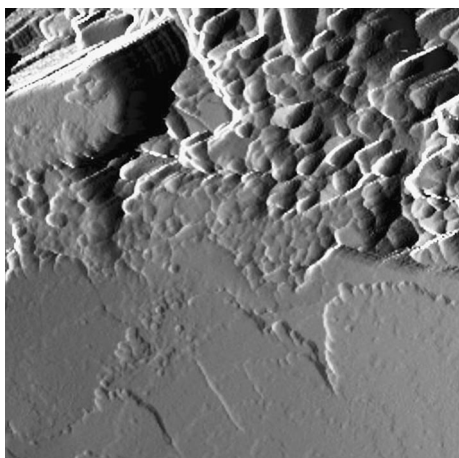
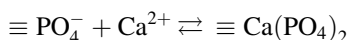
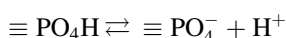
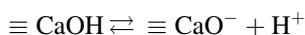
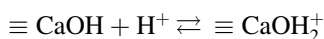


Fig. 1 Photo of hydroxyapatite surface made by AFM microscope

powders is different: higher grain density was obtained with powder A and B [8].

Hydroxyapatite is a salt so on its surface there are two kinds of groups; hydroxyl and phosphate ones. It can be assumed that similarly to acids, phosphate groups are definitely acidic but hydroxyl ones are amphoteric. The scheme of charge formation is presented by the reactions below:



Surface charge density of the studied sample of hydroxyapatite/aqueous solution of NaCl in function of pH shows that pH_{PZC} is equal to 7 but electrophoretic mobility measurements give $\text{pH}_{\text{IEP}} = 4$. Measurements of the surface charge and zeta potential for the hydroxyapatite/NaCl system were carried out in 25–37 °C, but no temperature influence has been observed. It is caused by too little temperature difference to observe any changes. For this

reason, the authors have placed the measurement outputs made in 25 °C.

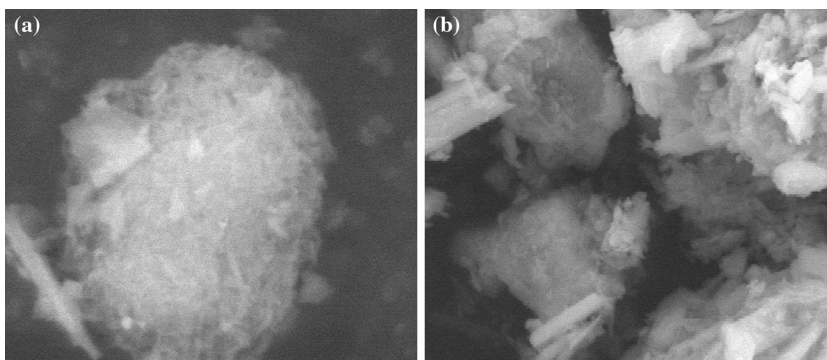
Smičiklas et al. [12], Bell et al. [13] and Janusz et al. [14] give the values of pH_{PZC} and pH_{IEP} for hydroxyapatite determined by potentiometric titration and electrophoresis in different basic electrolytes. Among the analysed values of pH_{PZC} and pH_{IEP} for individual samples, some are characterized by the values of $\text{pH}_{\text{IEP}} < 5$, whereas comparison of the values of pH_{PZC} is in the range 4.35–7 in different electrolytes. The obtained results are consistent with the literature.

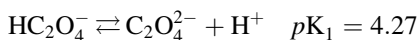
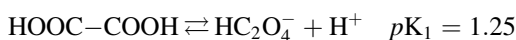
Dependence of surface charge density on pH allows to calculate the values of ionization and complexation equilibrium constants of surface hydroxyl groups. The constants were calculated as the fitting parameters for calculated model of ion adsorption reactions at the salt/electrolyte solution interface. Capacity has essential effect on the difference between the surface hydroxyl group ionization constants so $\Delta pK = pK_{a1} - pK_{a2}$. When the capacity value is about 0.5 F m^{-2} , the difference between the constants is small. Therefore, the values of equilibrium constants of reaction K, capacities C_1 , C_2 as well as density of surface groups must be taken into consideration together as a set of parameters. In the triplane model, these parameters were fitted by Hayes et al. [15], for the data from potentiometric titration (for different ionic forces). The values of equilibrium constants of ionization and complexation of surface groups present at the hydroxyapatite/electrolyte solution interface were calculated from the dependence of surface charge density on pH and load capacity electrolyte concentration. The data are presented in Table 2. Equilibrium constants of hydroxyl group surface reactions for individual systems were calculated using the Davis et al. [16] as well as Schwarzenbach modified methods [17].

Adsorption of oxalate ions

Oxalic acid is one of the strongest carboxylic acids in aqueous solutions and undergoes a two-stage dissociation. Its constants are [18]:

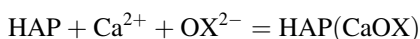
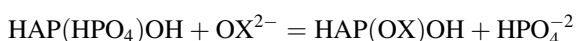
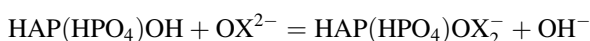
Fig. 2 **a** Photo of hydroxyapatite surface made by the STEM microscope. **b** Photo of hydroxyapatite/oxalic acid surface made by the STEM microscope





This is due to a mutual induction effect of two carboxylic groups. The contribution of ionic forms of oxalic acid in a pH function calculated from the equilibrium constants of the above-mentioned dissociation reaction is presented in Fig. 3.

In the pH range 1.5–3.9, the HC_2O_4^- form is predominant and above $\text{pH} = 4$ the $\text{C}_2\text{O}_4^{2-}$ form is predominant. As the investigations were carried out in the pH range 5–11, the oxalate anion may adsorb mainly as $\text{C}_2\text{O}_4^{2-}$. Adsorption of oxalate ions at the hydroxyapatite electrolyte solution interface can proceed according to the reactions:



The author believes that this process consists of two stages—the fast and slow ones. The slow stage is associated with the presence of natural 0.5-nm-diameter microchannels in the hydroxyapatite lattice through which electrolyte ions can interchange with the hydroxyapatite crystal lattice ions.

In order to determine mechanism of oxalate ions adsorption on hydroxyapatite, kinetics of phosphate ions concentration changes during the adsorption of oxalate ions was measured. As shown in Fig. 4, phosphate ions concentration increases with the progress of oxalate ions adsorption. However, the concentration growth is smaller than the change of phosphate ions concentration. This is the evidence that only a part of phosphate ions is exchanged into oxalate ones and the other part of adsorbing ions can exchange hydroxyl ions or undergo surface precipitation with calcium ions. Recrystallization of hydroxyapatite into calcium oxalate is possible in solutions with pH lower than 7.5. Under these conditions, calcium oxalate is a salt less soluble than hydroxyapatite Fig. 5.

Adsorption of oxalates at the hydroxyapatite/0.001 mol dm^{-3} NaCl electrolyte solution interface was measured using the method of radioactive oxalate ions

Table 2 Ionization and complexation equilibrium constants for the hydroxyapatite/NaCl system

| Constants | Davis et al. method | Schwarzenbach modified method |
|-----------|---------------------|-------------------------------|
| pK_{a1} | 5.76 | 5.59 |
| pK_{a2} | 9.91 | – |
| pK_{Cl} | 5.43 | 5.82 |
| pK_{Na} | 7.19 | 7.15 |

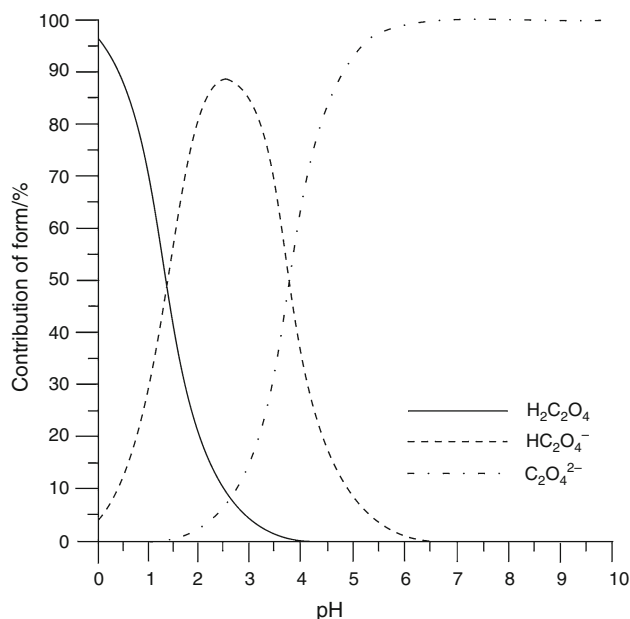


Fig. 3 Contribution of oxalate ions in a pH function

loss without taking into account diffusion in short time intervals. This indicates that the observed adsorption process was connected with exchange of ions on the surface but not deep inside the crystal which is conditioned by a natural process of ions exchange in the crystal lattice channels. Figures 6–9 below present the dependence of oxalate ions adsorption density at the hydroxyapatite/electrolyte solution interface as well as the diagram of equilibrium concentration of oxalate ions in solution in a pH function for the oxalate

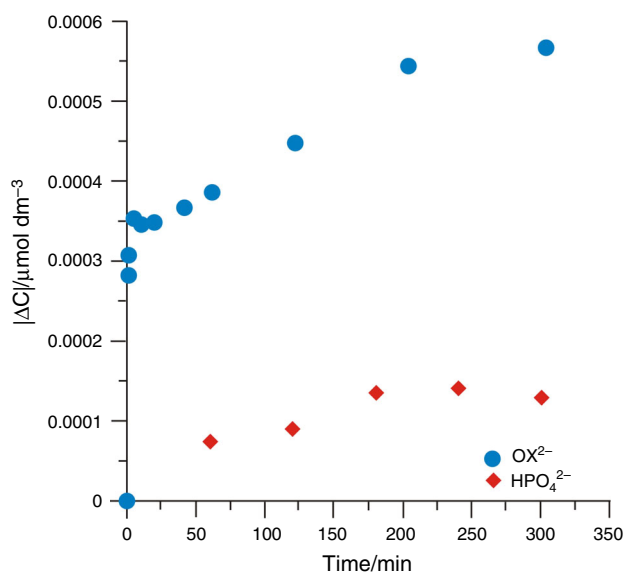


Fig. 4 Kinetic of adsorption

ions concentrations 0.000001 , 0.00001 , 0.0001 and $0.001 \text{ mol dm}^{-3}$.

As can be seen, adsorption of oxalate ions decreases with the increasing pH which is due to almost complete transition of these ions from the solution on the hydroxyapatite surface but over $\text{pH} = 9$ drop in oxalate adsorption is observed. Dependence of anions adsorption on hydroxyapatite proves that not only hydroxyl groups but also phosphate ones and the recrystallization process are responsible for adsorption. For the initial concentration of oxalate ions $0.000001 \text{ mol dm}^{-3}$ at $\text{pH} = 6.5$, it is about 50–60 %. pH plays an important role in the adsorption process affecting the surface charge of the adsorbent, ionization degree and adsorbate speciation. Thus, adsorption of oxalic acid on hydroxyapatite was studied in the pH range 3–11. The results are presented in Fig. 4. Adsorption capacity of the acid decreased, with the increasing pH it adsorbed poorly at $\text{pH} > 9$. At low pH, neutralization of negative charge on the adsorbent surface and increased protonation resulted in high adsorption of organic acids on hydroxyapatite. This facilitated diffusion and increased a number of active sites on the adsorbent surface, thus increasing adsorption. On the other hand, with the increasing pH, there was observed oxalic acid deprotonation which inhibited diffusion. The amount of adsorbed oxalic acid was reduced. Moreover, when solution pH is higher than pH_{PZC} of hydroxyapatite, the potential surface of hydroxyapatite is negative which increases electrostatic repulsion

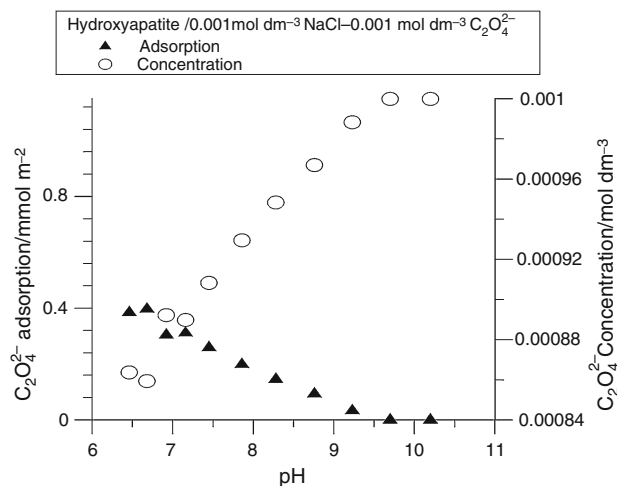


Fig. 6 Dependence of $\text{C}_2\text{O}_4^{2-}$ adsorption density on pH for the hydroxyapatite/ $0.001 \text{ mol dm}^{-3} \text{ NaCl}/0.001 \text{ mol dm}^{-3} \text{ C}_2\text{O}_4^{2-}$

between the negatively charged surface and oxalate ions resulting in lower adsorption on hydroxyapatite. Polar inorganic materials of hydroxyapatite type, which have a relatively high affinity for polar organic molecules of oxalic acid type, can form chemical bonds with them. Adsorption capacity of oxalic acid on hydroxyapatite depends on its polarization and ability of coordination with the surface, particularly with calcium ions. Highly polar oxalic acid can be adsorbed by hydroxyapatite due to strong coordination with calcium ions on the surface.

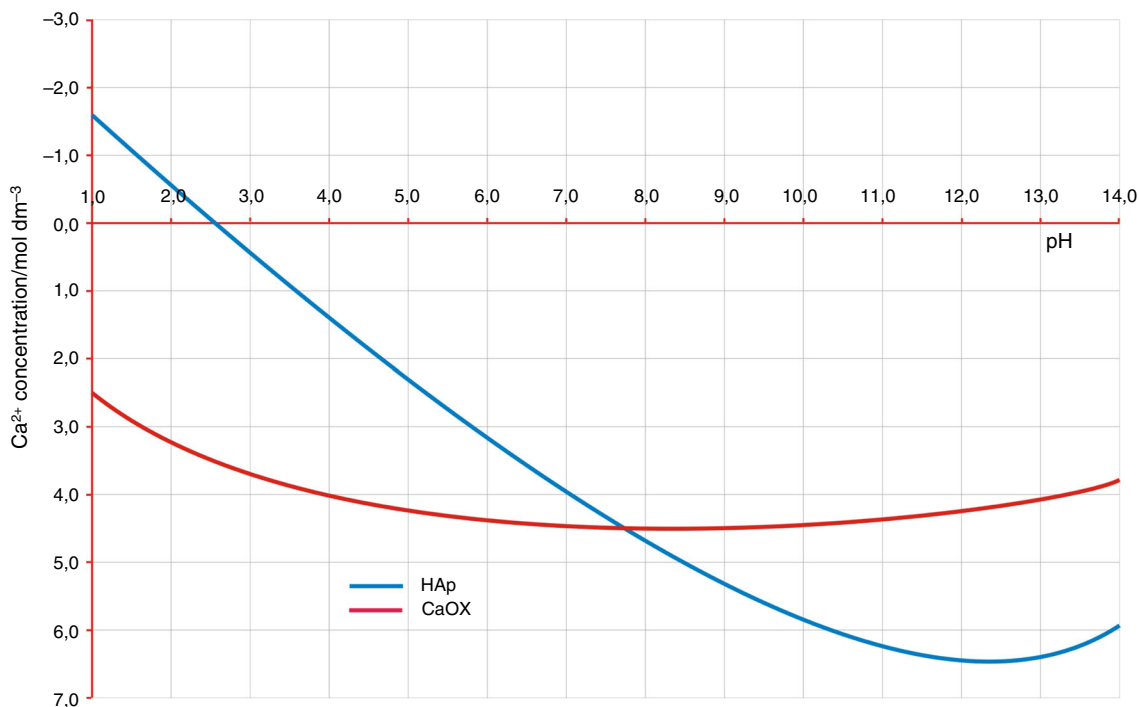


Fig. 5 Dissolved of hydroxyapatite and oxalic calcium

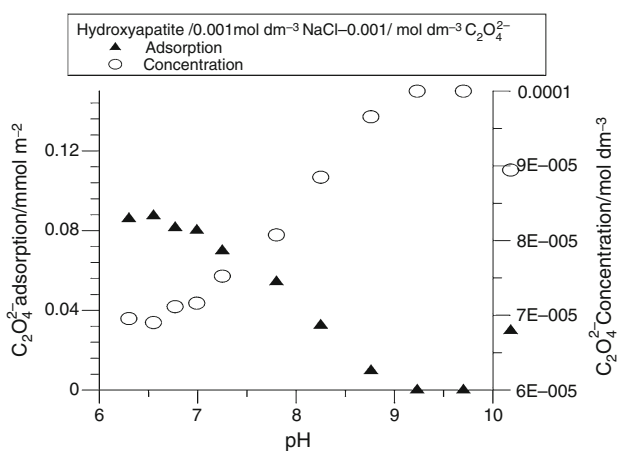


Fig. 7 Dependence of $C_2O_4^{2-}$ adsorption density on pH for the hydroxyapatite/ $0.001 \text{ mol dm}^{-3} \text{ NaCl}/0.0001 \text{ mol dm}^{-3} C_2O_4^{2-}$

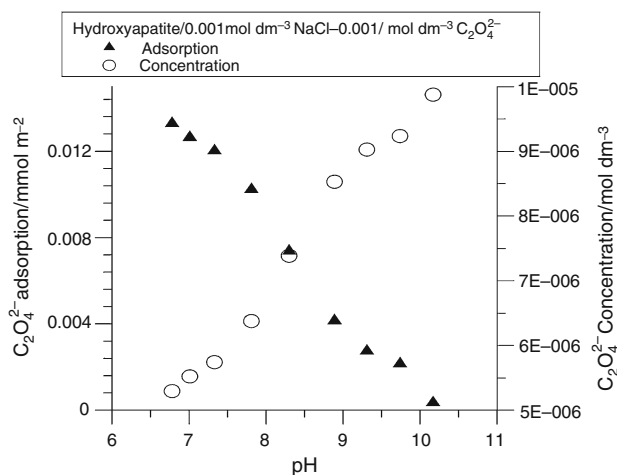


Fig. 8 Dependence of $C_2O_4^{2-}$ adsorption density on pH for the hydroxyapatite/ $0.001 \text{ mol dm}^{-3} \text{ NaCl}/0.00001 \text{ mol dm}^{-3} C_2O_4^{2-}$

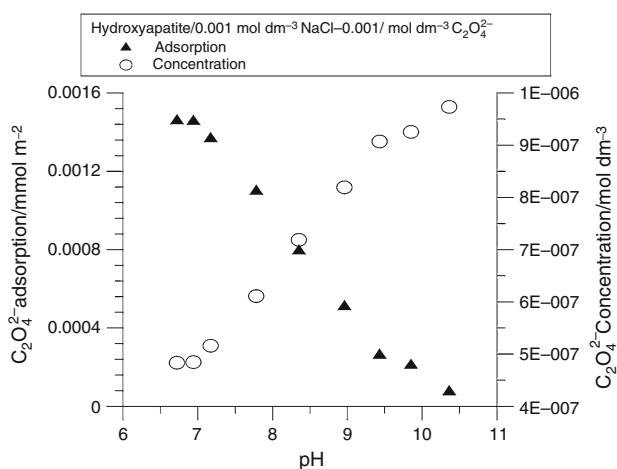


Fig. 9 Dependence of $C_2O_4^{2-}$ adsorption density on pH for the hydroxyapatite/ $0.001 \text{ mol dm}^{-3} \text{ NaCl}/0.000001 \text{ mol dm}^{-3} C_2O_4^{2-}$

Figure 10 presents the effect of basic electrolyte concentration on adsorption of oxalate ions in a pH function on the hydroxyapatite surface. As can be seen, a hundred times bigger concentration of basic electrolyte changes adsorption of oxalate ions in a complex way. In the pH range from 6 to 7 with the increasing NaCl concentration, adsorption diminishes due to reduced activity of oxalate ions in solution. However, the increase over pH 7.5 cannot be explained in this way. It seems that increase can be caused by weaker electrostatic interactions between oxalate anions and the negatively charged hydroxyapatite surface. Increase in the neutral electrolyte concentration favours desorption to a small extent. This can indicate that oxalate ions adsorb very strongly on the adsorbent surface and chloride ions can compete for adsorption sites despite large concentration.

Figure 11 presents dependence of adsorption of oxalate ions from the solution of the initial concentration $0.001 \text{ mol dm}^{-3}$ on the hydroxyapatite sample which was preliminarily conditioned at different time: 5 min, 14 h, 72 h. As can be seen, longer time of sample conditioning in the oxalate solution leads to only partial desorption of oxalate with the increasing pH value. This effect is caused by diffusion of oxalate ions through the hydroxyapatite channels deep inside the hydroxyapatite crystal. Quick desorption causes exchange of oxalate ions into hydroxylate ones only of those adsorbed on the surface of hydroxyapatite ions. Adsorption and structural properties of hydroxyapatite depend on the modification method. Figure 12a–c shows the thermal analysis of the samples adsorbed with oxalic acid on hydroxyapatite in various lengths of time: 5 min, 14 h, 72 h. From the TG and DTG

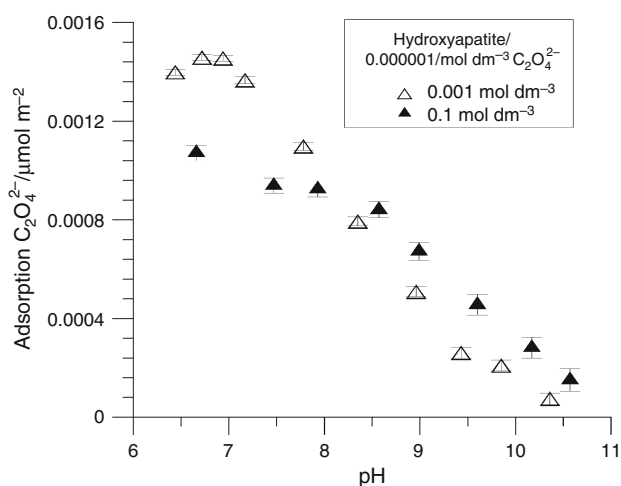


Fig. 10 Effect of NaCl electrolyte concentration on ions adsorption in a pH function for the hydroxyapatite/ $\text{NaCl}/0.000001 \text{ mol dm}^{-3} C_2O_4^{2-}$

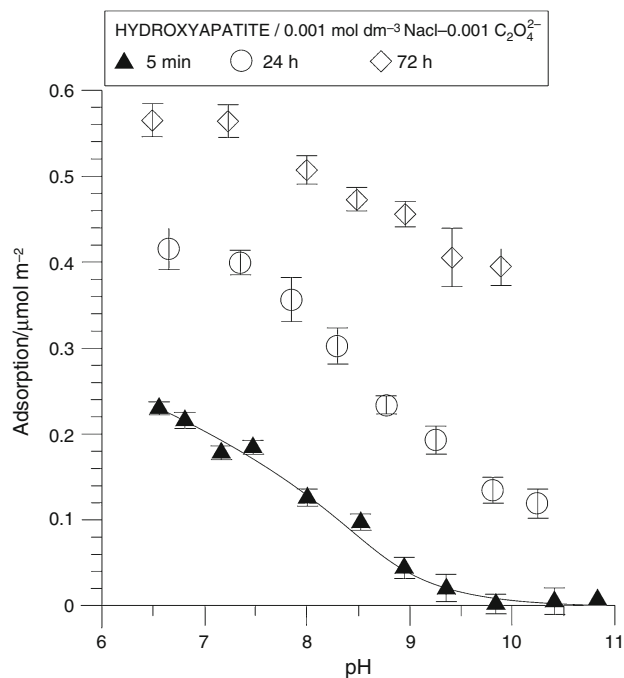


Fig. 11 Presents dependence of adsorption of oxalate ions from the solution of the initial concentration $0.001 \text{ mol dm}^{-3}$ on the hydroxyapatite

curves, it can be stated that due to heating of hydroxyapatite samples with adsorbed oxalic acid in the temperature range $20\text{--}950 \text{ }^\circ\text{C}$, there two stages can be distinguished connected with a small mass loss from 12 mg for a and c samples up to 13 mg for sample 2. In the temperature range, $20\text{--}200 \text{ }^\circ\text{C}$ mass loss with the minimum at about $80 \text{ }^\circ\text{C}$ is connected with the process of removal of hygroscopic water and that physically adsorbed on the surface of the studied hydroxyapatite and oxalic acid system. Melting point of oxalic acid is $189 \text{ }^\circ\text{C}$, heating oxalic acid causes its decarboxylation and transformation into formic acid. Under the influence of oxidizing agents, oxalic acid decomposes into carbon dioxide and water. Therefore, mass loss in this range of temperature is larger compared to that for pure hydroxyapatite described by Skwarek et al. [19]. In the temperature range $200\text{--}950 \text{ }^\circ\text{C}$, small mass loss results from removal of carbonates and chemically bonded water [20, 21]. These data are in agreement with the results obtained by Bianco et al. [22]. Adsorption of oxalic acid on hydroxyapatite not only changes active centres on the surface and their energies but also affects their thermal stability. From the DTG curves, there can be distinguished three stages of thermal decomposition. In the temperature range, $0\text{--}200 \text{ }^\circ\text{C}$ water and oxalic acid groups weakly coordinated on the surface are removed. In the second stage in the temperature range $200\text{--}400 \text{ }^\circ\text{C}$, mass loss on the TG curve in the cases with a distinct peak on the DTG curve with the minimum at $300 \text{ }^\circ\text{C}$ for all groups is connected

with release and oxidation of strongly bonded organic groups. In the $400\text{--}950 \text{ }^\circ\text{C}$ range, oxidation of organic carbon to CO_2 occurs which indicates formation of surface complexes between molecules of oxalic acid and hydroxyapatite and complexity of the whole process. Drop in peaks intensity in the temperature ranges $20\text{--}200$, $200\text{--}400$ and $400\text{--}800 \text{ }^\circ\text{C}$ points out to an increase in interaction forces between the hydroxyapatite surface and oxalic acid molecules.

Figure 13 presents the percentage dependence of oxalate ions adsorption at the hydroxyapatite/ $0.001 \text{ mol dm}^{-3}$ NaCl solution interface. As can be seen, adsorption does not reach 100 % in any system, and at the lowest concentrations it reaches only 50 %; therefore, it is difficult to determine such adsorption parameters as $\text{pH}_{50\%}$ or $\text{pH}_{10\text{--}90\%}$. However, it can be stated that the envelope changes its position with the change of oxalate ions concentration in the system. The lower the concentration of anions, the steeper the edge is and shifts towards alkaline values.

Influence of adsorption on the changes of H^+/OH^- ions concentration in the hydroxyapatite/ $0.001 \text{ mol dm}^{-3}$ NaCl electrolyte solution is presented in Fig. 14. As can be seen, no changes are observed in the course of the dependence of surface charge density on pH. Only for the initial concentrations $0.001 \text{ mol dm}^{-3}$ at pH over 8 of oxalate, there is observed hydroxyl ions release which is observed with the pH increase. As adsorption of oxalate ions is the highest at $\text{pH} = 6$, the release of oxalate ions can accelerate change of hydroxyapatite surface character replacing OH and HPO_4 groups of lower acidity with the oxalic ones which exhibit more acidic character. The effect of oxalate ions on the zeta potential is presented in Fig. 15. There can be observed a rapid drop of the zeta potential starting with the concentration $0.000001 \text{ mol dm}^{-3}$, which may result from overcharging of the compact electrical double layer (edl) or increase of concentration negatively charged groups on the hydroxyapatite surface (dissociation of adsorbed hydrogen oxalate). For the studied system at the same $\text{pH} = 5$, the potential value difference is -15 mV , for the $0.001 \text{ mol dm}^{-3}$ electrolyte -7 mV and for the oxalate samples -22 mV . The increase of initial oxalate ions concentration up to $0.001 \text{ mol dm}^{-3}$ leads to further decrease of zeta potential. Oxalate ions change the character of hydroxyapatite surface-increase its acidic character. This is most probably caused by the formation of intraspherical complexes due to oxalate adsorption.

By definition, the isoelectric point (IEP) is at pH when the charge from all sources is zero, while the point of zero charge (PZC) is at pH when the net adsorption density of H^+ and OH^- is zero. Operationally, the IEP can be regarded as the pH when the ζ potential is zero [23]. To determine the values of parameters of sample surface

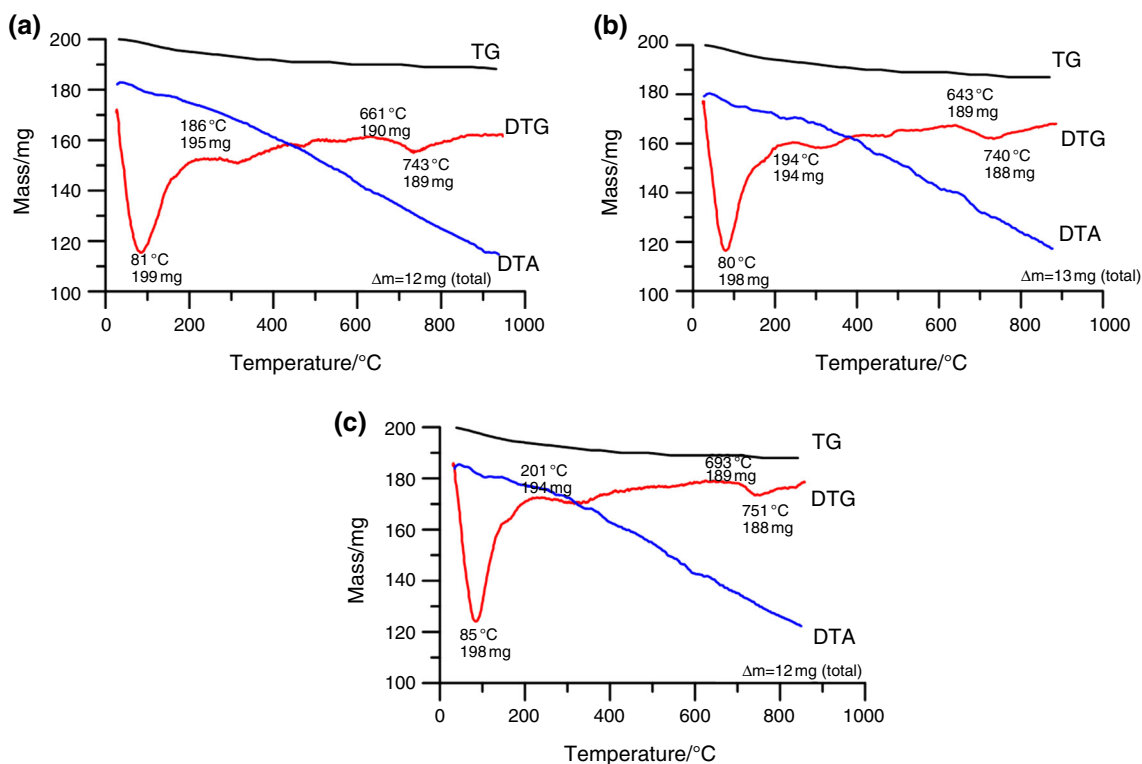


Fig. 12 Results of thermogravimetric analysis

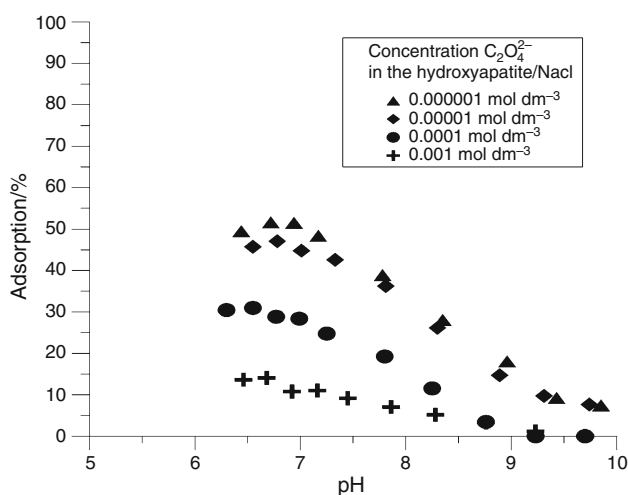


Fig. 13 Dependence of $C_2O_4^{2-}$ adsorption on pH for the hydroxyapatite/ $0.001 \text{ mol dm}^{-3} \text{ NaCl}/C_2O_4^{2-}$ system

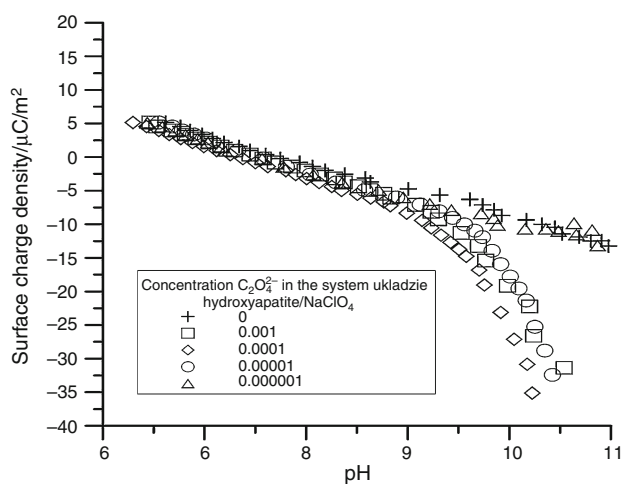


Fig. 14 Change of H^+/OH ions concentration in the hydroxyapatite/ 0.001 NaCl solution system affected by oxalate ions adsorption

porous structure, there was applied a well-known and often used a low-temperature nitrogen adsorption–desorption (Table 3). Recrystallization caused by different solubility of hydroxyapatite and calcium oxalate is one of the oxalate ions adsorption mechanisms. For testing it, the sample surface area was measured after oxalate ions adsorption from the solution of the initial concentration $0.001 \text{ mol dm}^{-3}$. As can be seen, adsorption of oxalates

results in the specific surface area decrease by $12 \text{ m}^2 \text{ g}^{-1}$, with the simultaneous increase of average pore radius from 13.21 to 20.69 nm. These changes are caused by lower contribution of small pores in the sample.

The data in Fig. 16 presenting the differential pore distribution indicate that hydroxyapatites contain mainly micropores. After oxalic acid adsorption, the number of mesopores increased and that of micropores decreased

which is in agreement with the results presented in table earlier.

The comparison of grain distribution of hydroxyapatite samples before and during adsorption for the initial oxalate concentration $0.001 \text{ mol dm}^{-3}$ is given in Fig. 17. As can be seen, after the addition of oxalates, there is found dissolution of some fine $1\text{--}2 \mu\text{m}$ molecules and increase of larger $3\text{--}10 \mu\text{m}$ molecules contribution. This phenomenon is confirmed by the recrystallization mechanism.

In this work, stability measurements from the turbiscan have been added:

- hydroxyapatite/ $0.001 \text{ mol dm}^{-3}$ NaCl in $25 \text{ }^\circ\text{C}$ i $37 \text{ }^\circ\text{C}$,
- hydroxyapatite/ $0.001 \text{ mol dm}^{-3}$ NaCl/ $0.001 \text{ mol dm}^{-3}$ oxalic acid in $25 \text{ }^\circ\text{C}$.

As it can be seen from Fig. 18, on the bottom of the measurement flask sedimentation occurs. The dynamics of this sediment generation is quite big, and differences can be observed between the first and next scans. The suspension there is unstable, and flocculation occurs. Its dynamics raises, which can be read from scanning, and then goes down—differences between scans are smaller. In the

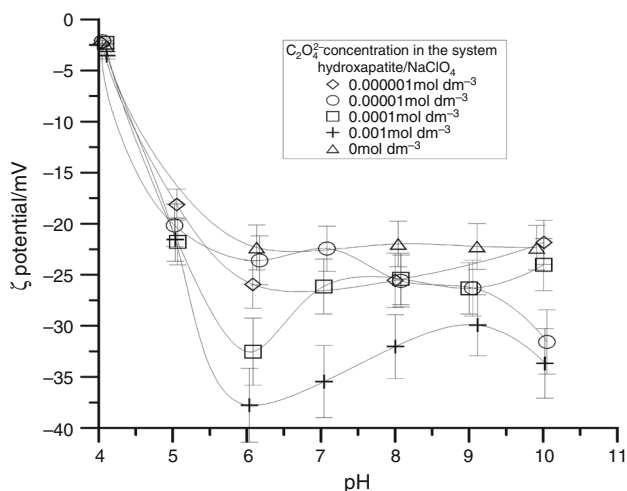


Fig. 15 Dependence of zeta potential in a function of pH and electrolyte concentration for the hydroxyapatite/ $0.001 \text{ mol dm}^{-3}$ NaCl/ $\text{C}_2\text{O}_4^{2-}$ system

Table 3 Some structural parameters of hydroxyapatite

| | HAP | HAP/oxalic acid |
|--|------|-----------------|
| Surface area from BET m^2/g | 35.4 | 23.2 |
| Surface area from Langmuir isotherm m^2/g | 50.2 | 34.4 |
| Total pore volume from adsorption $1.7 \text{ nm} < d < 300 \text{ nm}$ by BJH method cm^3/g | 0.1 | 0.1 |
| Total pore volume from desorption $1.7 \text{ nm} < d < 300 \text{ nm}$ by BJH method cm^3/g | 0.1 | 0.1 |
| Average pores radius from BET method nm | 13.2 | 20.7 |
| Average pores radius from adsorption, BJH method nm | 12.5 | 20.7 |
| Average pores radius from desorption, BJH method nm | 8.7 | 20.7 |

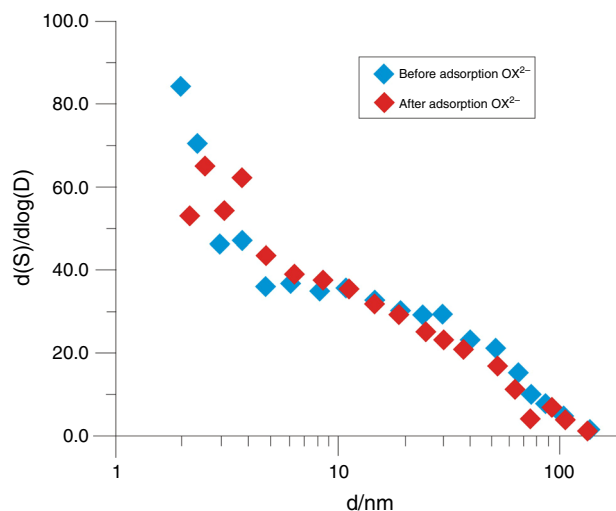


Fig. 16 Pours in hydroxyapatite before and after adsorption

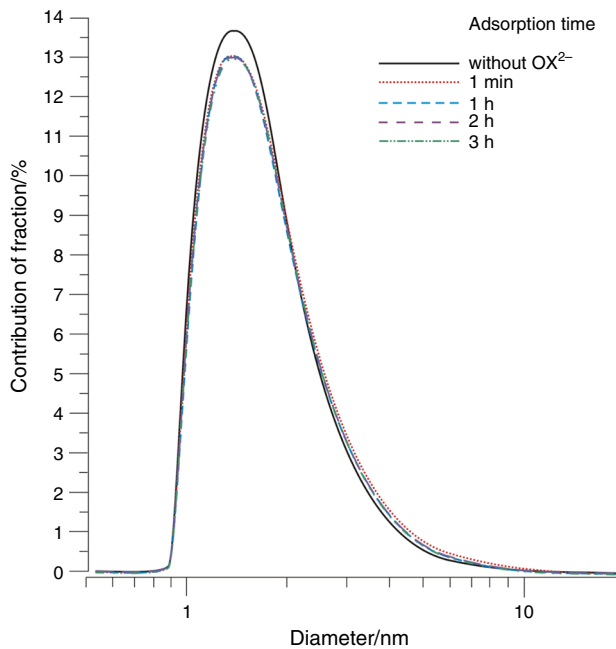


Fig. 17 Grain dimensions of hydroxyapatite before and after adsorption

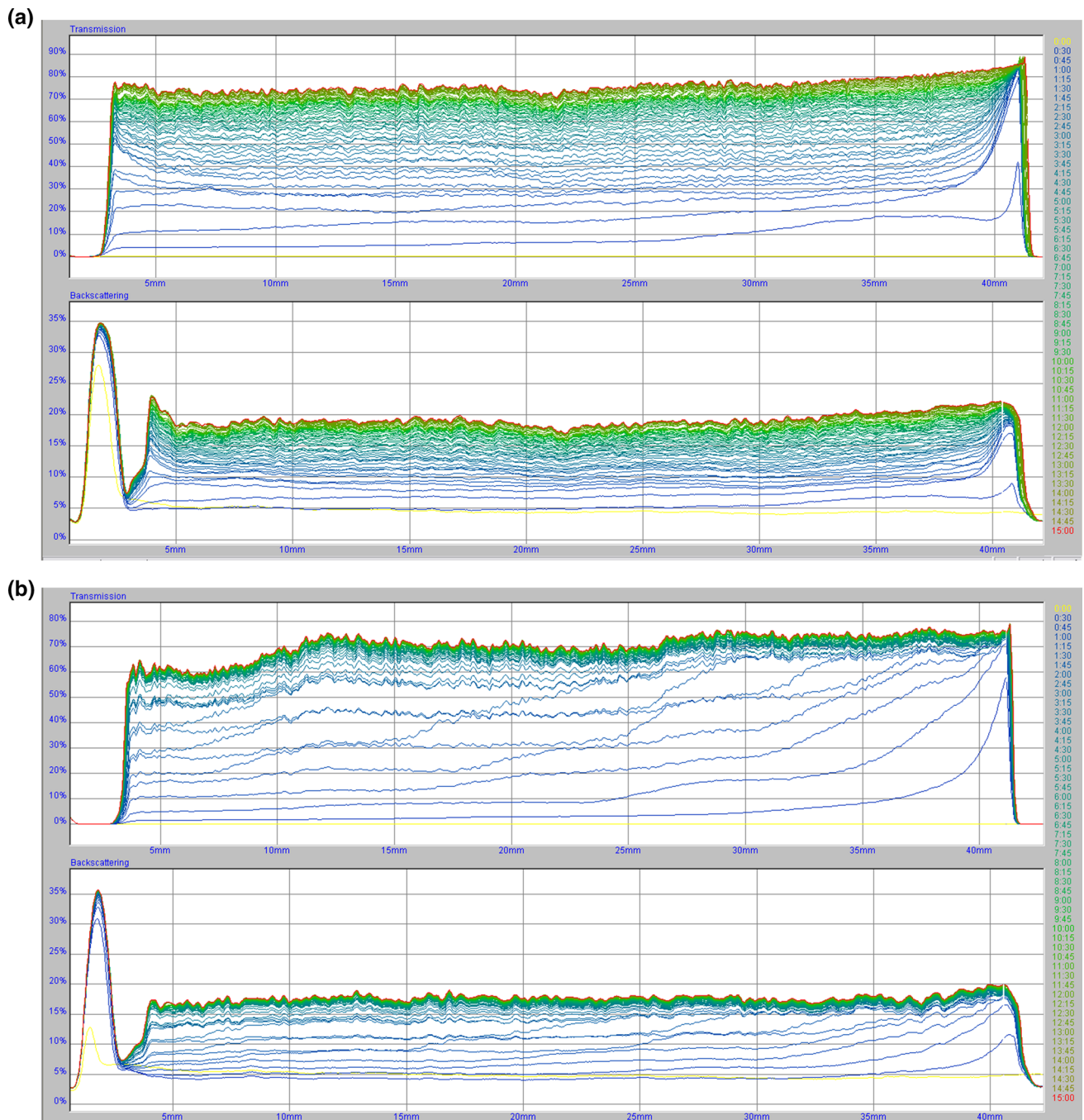


Fig. 18 Transmission and backscattering curves for systems: **a** HAP/ $0.001 \text{ mol dm}^{-3} \text{ NaCl}/25 \text{ }^\circ\text{C}$, **b** HAP/ $0.001 \text{ mol dm}^{-3} \text{ NaCl}/37 \text{ }^\circ\text{C}$ **c** HAP/ $0.001 \text{ mol dm}^{-3} \text{ NaCl}/0.001 \text{ mol dm}^{-3} \text{ oxalic acid}$. The level

of suspension in the measurement vial is along the x -axis, and the light intensity [%] transmitted through the suspension or backscattered on the solid particles is along the y -axis

sample of hydroxyapatite/ $0.001 \text{ mol dm}^{-3} \text{ NaCl}$ in $37 \text{ }^\circ\text{C}$, sedimentation layer creates at once and stratifies slightly during the measurement. The dynamic flocculation exists

there, which can be proved by unified stratification of next scans. Sample 1 is similar to 3 so in $25 \text{ }^\circ\text{C}$ oxalic acid presence does not influence the system stability.

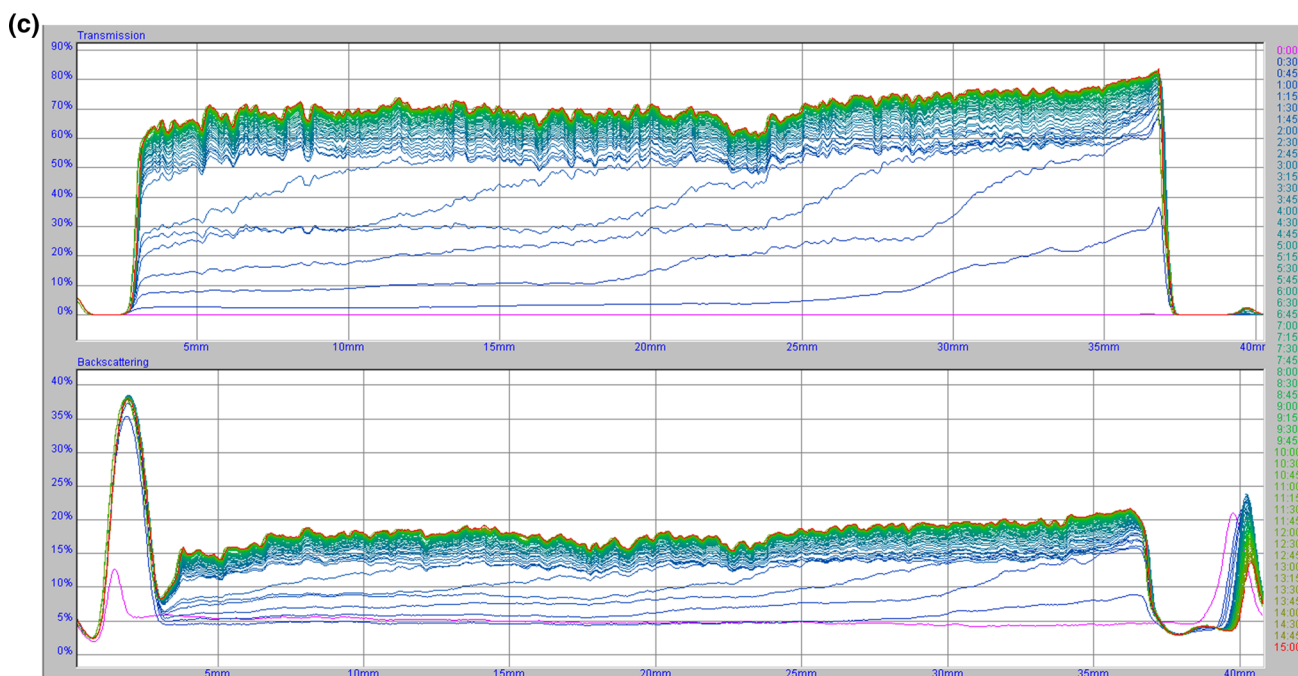


Fig. 18 continued

Conclusions

The results of investigations on $\text{C}_2\text{O}_4^{2-}$ ions adsorption at the hydroxyapatite/NaCl interface are as follows: hydroxyapatite was prepared by the hydrothermal method using CaHPO_4 and $\text{Ca}(\text{OH})_2$. The surfaces of the obtained hydroxyapatite were characterized using the following methods: XRD, AFM, SEM, nitrogen adsorption/desorption. The spectra characteristic of hydroxyapatite was obtained. Due to mineral solubility, measurements of ions adsorption in the hydroxyapatite/electrolyte solution system are limited to the pH range 6–10. The values characteristic of the double electrical layer for the obtained compound are $\text{pH}_{\text{PZC}} = 7$, $\text{pH}_{\text{IEP}} = 4$.

Adsorption of $\text{C}_2\text{O}_4^{2-}$ ions on the surface increases with the increasing pH and is characterized by the envelope whose position with the increasing concentration of oxalate ions shifts towards higher pH values and its slope decreases. Extension of conditioning time of the hydroxyapatite sample in the oxalate solution leads to only particle desorption of oxalate with the increasing pH. The presence of oxalic acid causes zeta potential drop which is visible for the initial concentration $0.001 \text{ mol dm}^{-3}$ of oxalates. Decrease in peaks intensity in the temperature range 20–200, 200–400 and 400–800 °C points out to the increase in interactions between the hydroxyapatite surface and oxalic acid molecules. Adsorption of oxalic acid occurs as a result of replacement of the phosphate groups on the hydroxyapatite surface with the oxalic ones together with

the formation of intraspherical complexes. This phenomenon is confirmed by the recrystallization mechanism.

Acknowledgements The author is grateful to Dariusz Sternik for making thermal analysis measurements for the studied systems.

Open Access This article is distributed under the terms of the Creative Commons Attribution 4.0 International License (<http://creativecommons.org/licenses/by/4.0/>), which permits unrestricted use, distribution, and reproduction in any medium, provided you give appropriate credit to the original author(s) and the source, provide a link to the Creative Commons license, and indicate if changes were made.

References

1. Wang YJ. Effects of low-molecular-weight organic acids on Cu (II) adsorption onto hydroxyapatite nanoparticles. *J Hazard Mater.* 2009;162:1135–42.
2. Wei W, Sun R, Wei ZG, Zhao HY, Li HX, Hu F. Elimination of the interference from nitrate ions on oxalic acid in RP-HPLC by solid-phase extraction with nanosized hydroxyapatite. *J Liq Chromatogr Related Technol.* 2009;32:106–24.
3. Wang Y, Chen NP, Wei W, Cui J, Wei ZG. Enhanced adsorption of fluoride from aqueous solution onto nanosized hydroxyapatite by low-molecular weight organic acids. *Desalination.* 2011;276:161–8.
4. Wei W. Interaction between low molecular weight organic acids and hydroxyapatite with different degrees of crystallinity. *Colloids Surf A.* 2011;392:67–75.
5. Adamczyk Z., Jaszczólt K., Jachimska B., Nattich M. Determination of Physicochemical properties and the thermal stability of hydroxyapatite. *Prace instytutu Odlewnictwa* 2008; XLVIII: Zeszyt 1.
6. Tõnsuaadu K, Gross KA, Plüdüma L, Veiderma M. A review on the thermal stability of calcium apatites. *J Therm Anal Calorim.* 2012;110(2):647–59.

7. Kohutova A, Honcova P, Svoboda L, Bezdička P, Maříkova M. Structural characterization and thermal behaviour of biological hydroxyapatite. *J Therm Anal Calorim.* 2012;108:163–70.
8. Mezahi FZ, Oudadesse H, Harabi A, Lucas-Girot A, Le Gal Y, Chaair H, Cathelineau G. Dissolution kinetic and structural behaviour of natural hydroxyapatite vs. thermal treatment Comparison to synthetic hydroxyapatite. *J Therm Anal Calorim.* 2009;959(1):21–9.
9. Landi E, Tampieri A, Celotti G, Sprio S. Densification behaviour and mechanisms of synthetic hydroxyapatite. *J Eur Ceram Soc.* 2000;20:2377–87.
10. Harding IS, Rashid N, Hing K. A Surface charge and the effect of excess calcium ions on the hydroxyapatite surface. *Biomaterials.* 2005;26:6818–26.
11. Dean-Mo L. Fabrication and characterization of porous hydroxyapatite granules. *Biomaterials.* 1996;17:1955–7.
12. Smiciklas ID, Milonjic SK, Pfindt P, Raicević S. The point of zero charge and sorption of cadmium (II) and strontium (II) ions on synthetic hydroxyapatite. *Sep Purif Technol.* 2000;18:185–93.
13. Bell LC, Posner AM, Quirk JP. The point of zero charge of hydroxyapatite and fluorapatite in aqueous solutions. *J Colloid Interface Sci.* 1973;42:250–9.
14. Janusz W, Skwarek E, Zlotucha A, Reszka M. The electric double layer at the hydroxyapatite/ NaClO_4 solution interface. *Polish J Chem.* 2008;82:57–67.
15. Hayes KF, Redden G, Ela W, Leckie JO. Surface complexation models: an evaluation of model parameter. *J Colloid Interface Sci.* 1991;142(448–5):6.
16. Davis JA, James O, Leckie O. Surface ionization and complexation at the oxide/water interface. I. Computation of electrical double layer properties in simple electrolytes. *J Colloid Interface Sci.* 1978;63:480–9.
17. Janusz W. Determination of surface ionization and complexation constants from potentiometric titration data Polish. *J Chem.* 1991;65:799–807.
18. http://tabelachemiczne.chemicalforum.eu/stale_dysocjacji.html.
19. Skwarek E, Janusz W, Sternik D. Adsorption of citrate ions on hydroxyapatite synthesized by various methods. *J Radioanal Nucl Chem.* 2014;299:2027–36.
20. Pang YX, Bao X. Influence of temperature, ripening time and calcination on the morphology and crystallinity of hydroxyapatite nanoparticles. *J Eur Ceram Soc.* 2003;23:1697–704.
21. Krajewski A, Mazzocchi M, Buldini PL, Ravaglioli A, Tinti A, Taddei P, Fagnano C. Synthesis of carbonated hydroxyapatites: efficiency of the substitution and critical evaluation of analytical methods. *J Mol Struct.* 2005;744–747:221–8.
22. Bianco A, Cacciotti I, Lombardi M, Montanaro L, Gusmano G. Thermal stability and sintering behaviour of hydroxyapatite nanopowders. *J Therm Anal Calorim.* 2007;88(1):237–43.
23. Renkou Xu, Li Chengbao, Ji Guoliang. Effect of low-molecular-weight organic anions on electrokinetic properties of variable charge soils. *J Colloid Interface Sci.* 2004;277:243–7.